EMPIRICAL GF-DETERMINATION FROM THE SOLAR SPECTRUM

Robert J. Rutten
Sterrewacht "Sonnenborgh", Utrecht, The Netherlands

Roman I. Kostik
Main Astronomical Observatory, Kiev, USSR

ABSTRACT. We test the reliability of Fe I and Fe II oscillator strengths determined empirically from optical solar lines by comparing fits of the observed line widths and line depths for various formation parameters.

1. INTRODUCTION

Ideally one uses precise oscillator strengths in any analysis requiring them. In practice, this is usually not possible. Fig. 1 illustrates this for iron abundance determination. The upper term diagram consists of Fe I lines for which precise oscillator strengths have been measured at Oxford (Blackwell et al. 1982 and references therein). The lower term diagram consists of actual solar Fe I lines suitable for abundance determination. The Oxford lines are mostly strong ultraviolet lines while in abundance determination one selects weak optical lines; the latter tend to lie higher in the term diagram. It would be better to use Fe II lines wherever Fe II is the dominant ionization stage, but Fe II lines have not been measured at Oxford.

Therefore a familiar recipe has been to derive empirical oscillator strengths form the solar spectrum. The classic example is Holweger's (1967) fitting of the equivalent widths of the stronger Fe I lines in the blue by adjusting their oscillator strengths, in order to derive his well-known LTE model photosphere from their observed depths. More recently, Gurtovenko and Kostik (1981a) used the updated version of this model (Holweger and Müller 1974, HOLMUL) to find the gf-values of the 865 solar Fe I lines shown in Fig. 1 by fitting their observed depths. For a smaller subset, they also fitted the equivalent widths (Gurtovenko and Kostik 1981b). The differences between the two fits were analysed by Rutten and Kostik (1982), and led to a NLTE formulation of the Fe I curve of growth by Rutten and Zwaan (1983). The latter was used by Rutten and Van der Zalm (1984) to compile 256 Fe I oscillator strengths from equivalent widths in the Jungfraujoch Atlas (Delbouille et al. 1973).

In this paper, we use line widths and line depths taken from

R. Viotti et al. (eds.), Physics of Formation of FeII Lines Outside LTE, 83–92.

Rutten and Van der Zalm (1984) for 354 Fe I lines and 22 Fe II lines which are all the clean iron lines present in the solar spectru between 4000 and 8000 Å. Since all parameters and assumptions of sola line formation enter into the reliability of solar-fitted oscillato strengths, we compare "gf_W" fits to the equivalent widths with "gf_D" fits to the depths of these lines for various combinations of inpu parameters. The resulting scatter diagrams provide a measure of th precision obtainable.

2. ATMOSPHERIC MODEL

Fig. 2 compares gf_D and gf_W LTE fits for two model atmospheres. Th HOLMUL model (top) is the favourite choice of LTE abundance deter miners because the spread it produces is smaller than when the well known HSRA model (Gingerich et al. 1971, bottom) is used. This i demonstrated by the difference between the top and bottom panels. Fit with the HSRA assuming LTE show increasing discrepancies between gf_D and gf_W for larger height of line formation, implying that the HSRA computed lines are too deep for their observed areas. This dept excess is due to the NLTE departures that go together with cool model as the HSRA (see Rutten, elsewhere in these proceedings). For Fe I assuming LTE results in too large computed line opacities, thus i line-core formation that is located too high, thus in too low line core brightness temperatures. For Fe II, assuming LTE produces too lo line source functions in the upper photosphere, thus too low line-cor brightness temperatures also.

The top panel of Fig. 3 shows that the discrepancies largel vanish when NLTE departures computed from the HSRA model are take into account. The bottom panel is for the recent MACKKL model (Maltb et al. 1986), which is close to the HOLMUL model in the upper photo sphere. Its concomitant NLTE departures are small; when taken int account (thanks to specification in a private communication by E. H Avrett), a scatter diagram results that is similar to the top panel This similarity demonstrates that the choice between either a ho model with small NLTE effects or a cool model with large NLT departures cannot be settled from the observed Fe I and Fe II lines.

3. CONTINUUM OPACITY

Figs. 4 and 5 display typical errors due to erroneous continuu intensities. They show results for an increase by 10% in the continu ous opacity, respectively for the line widths and for the line depths Experience learns that the continua produced by different spectru synthesis codes can differ by as much as 10%, even in the optica where H^- dominates. Also, most lines do not reach the "true" continuu but only a "local" continuum affected by unresolved weak lines and fa wings of nearby strong lines.

For Fe I lines, the differences in the fitted gf_W values ar smaller than the opacity increment (10% = 0.04 dex) for weak lines o

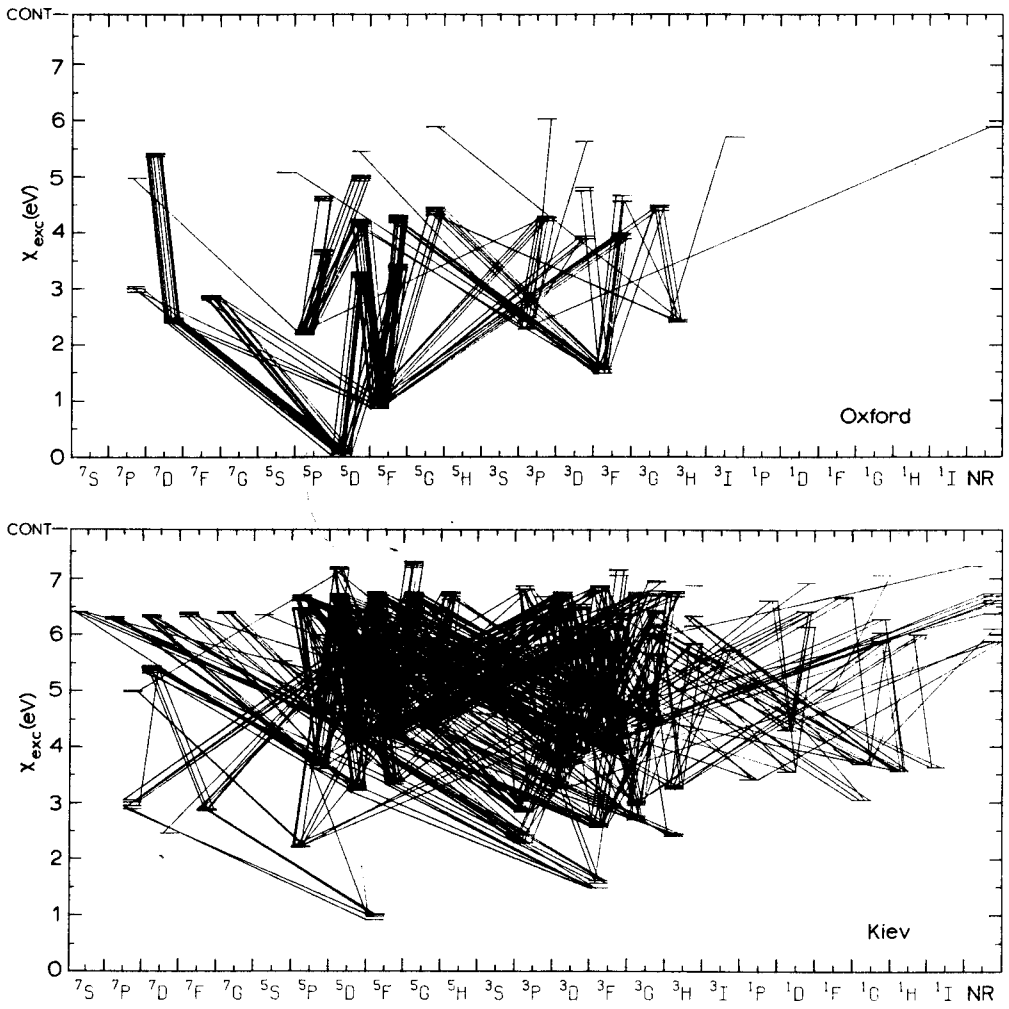

Fig. 1. Term diagrams for Fe I lines, respectively measured at Ox (top) and observable in the optical solar spectrum (bottom). Each label designates both the even-parity term (lefthand interval) and odd-parity term (righthand interval). Level designations are from RMT (Moore 1959); NR and NR° at right combine all number designat in the RMT.

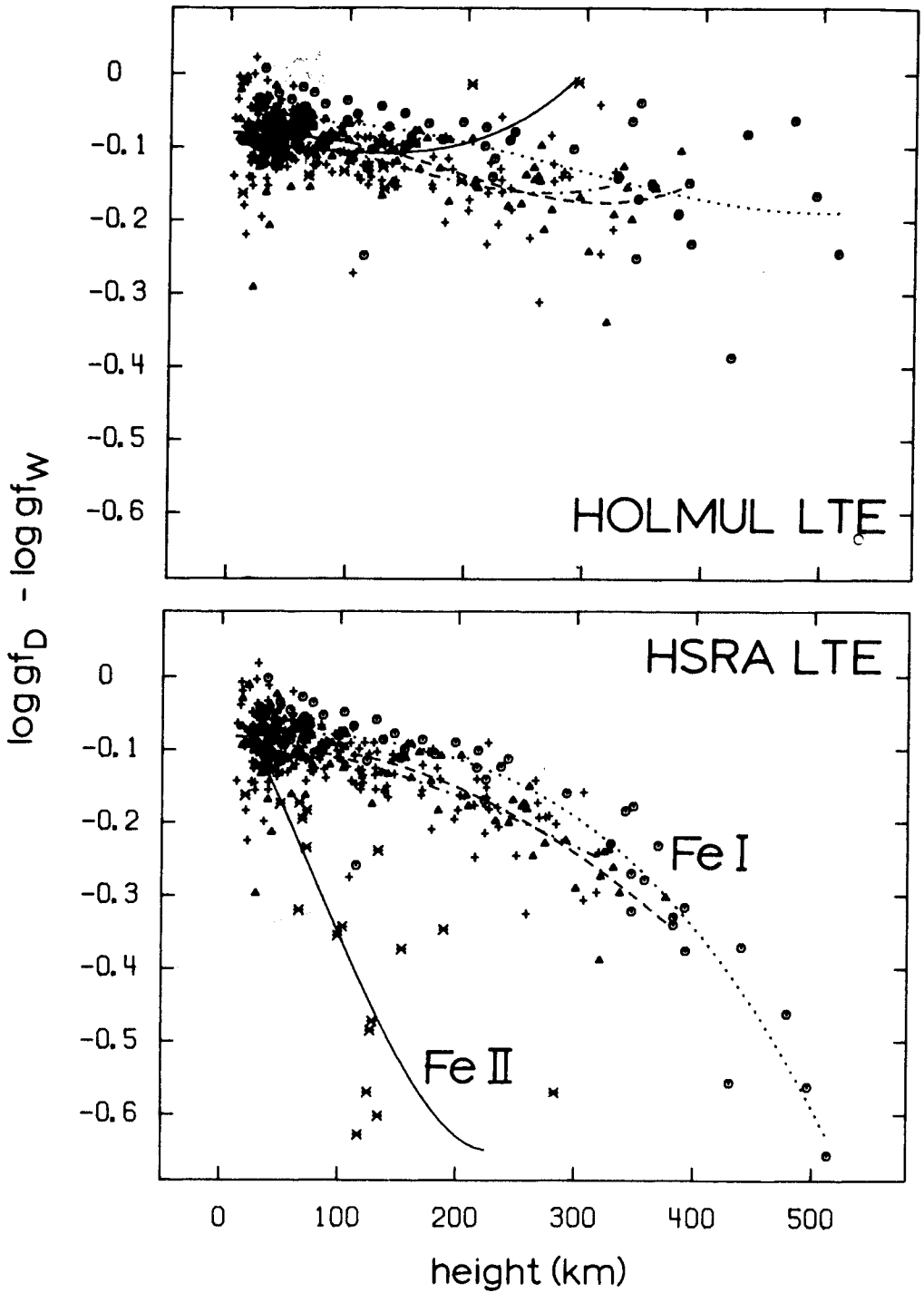

Fig. 2. Logarithmic differences between gf_W and gf_D for LTE model
against the line-center height of formation for the gf_W fit.
Fe II lines: asterisks, fitted with the solid curve.
Fe I lines: split into low excitation lines (circles, dotted f
middle excitation lines (triangles, dashed fit) and high excita
lines (plusses, dot-dashed fit) according to Rutten and Kostik (19
Microturbulence: MACKKL model. Macroturbulence: 1.3 km/s. Damp
radiative broadening and Van der Waals broadening computed
Warner's (1969) square radii and increased by 30%.

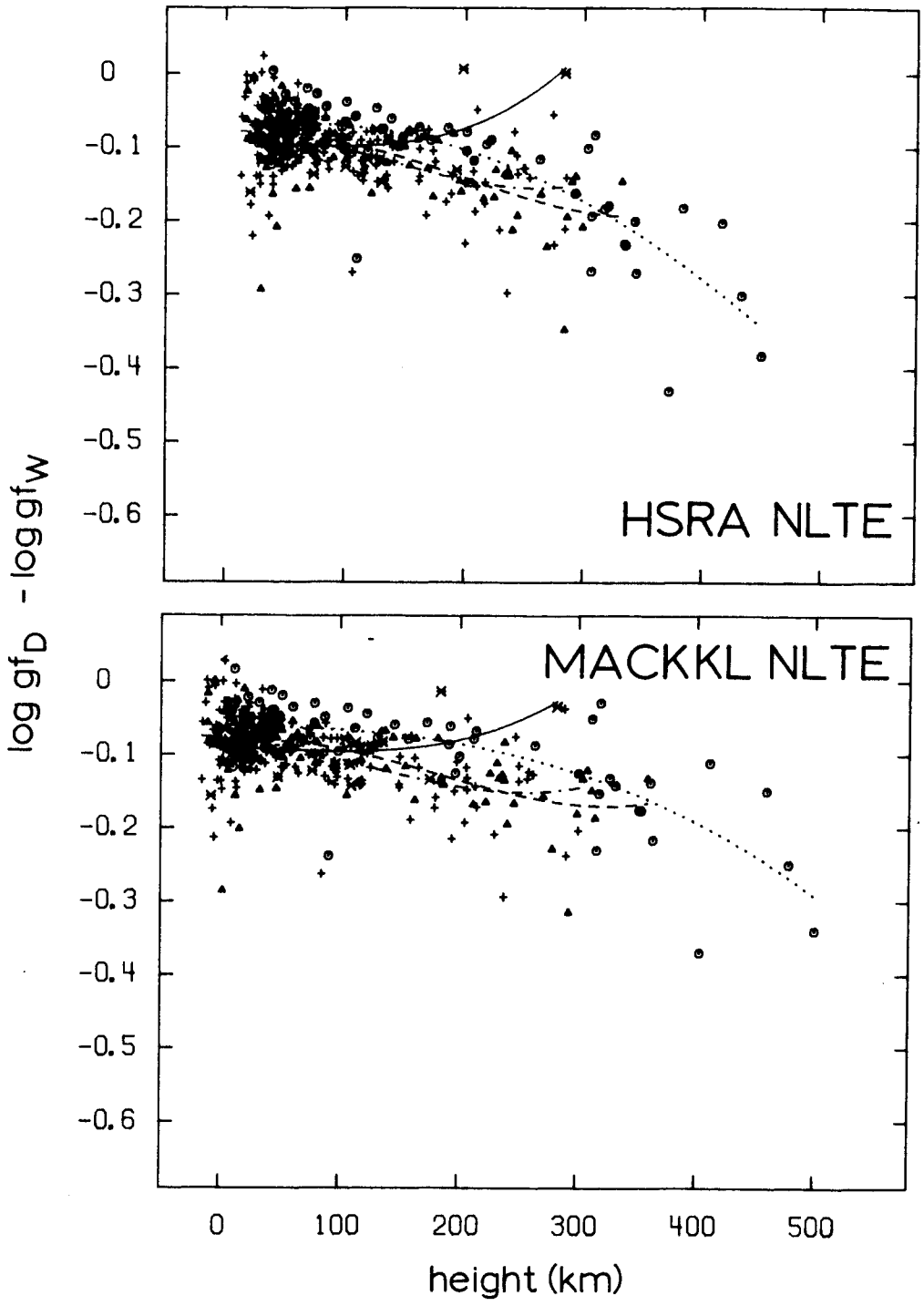

ig. 3. Logarithmic differences between gf_D and gf_W for NLTE odeling. Top: HSRA model, Fe I and Fe II NLTE departures as in Rutten nd Kostik (1982), taken from Lites and White (1973) and Cram et al. 1980), respectively.
ottom: MACKKL model; Fe I departures from Avrett, Fe II in LTE.
ymbol coding and other parameters as in Fig. 2.

the linear part of the curve of growth (log $W/\lambda < -5.5$, bottom panel Fig. 5). This is due to the rapid increase of the Fe I line extinction relative to the continuous extinction with height (Rutten and Van der Zalm 1984 Fig. 3). The Fe I increments computed here in LTE for the HOLMUL model are slightly larger than the values tabulated by Rutten and Van der Zalm for NLTE HSRA modeling[1)].

The differences increase with excitation energy at given formation height because for higher-excitation lines the outward increase in line-to-continuum extinction ratio is reduced by their larger sensitivity to the decreasing temperature. A reversed split is seen in the bottom panel of Fig. 4 against oscillator strength; it simply follows the Boltzmann population factor. This figure illustrates important selection effects. At high excitation, most lines selected for clean observability are already on the flat part of the curve of growth (upward curves here) and are therefore very sensitive to the turbulence parameters. The strongest high-excitation lines are the only optical Fe I lines with large transition probabilities. Their photon losses result in upper-level under- excitation and have led to overestimation of their gf-values by Gurtovenko and Kostik (1981a).

Fig. 5 shows the effects of increased continuous opacity on the line depths. The gf_D increments for weak lines are about the same as for the fits of the widths, but they are twice as large for lines from the shoulder of the curve of growth. They would be very large for saturated lines (log $W/\lambda > -4$), but such lines are not at all present when one selects clean solar lines.

4. TURBULENCE

Finally we show in Fig. 6 two examples in which the assumed turbulence differs. In the top panel we compare gf_D fits for the HOLMUL model and LTE, respectively with constant turbulence and with the height-dependent model specified in the MACKKL model (identical to the microturbulence in Vernazza, Avrett and Loeser 1976, 1981). In the bottom panel we compare gf_D fits using the height-dependent vertical microturbulence specified by Lites (1973) with fits using the MACKKL microturbulence, for the HSRA and NLTE. The differences in the top panel are large for the stronger lines which feel the outward decrease of the MACKKL microturbulence. The bottom panel shows large differences already for weak lines because Lites' microturbulence is quite large in the deep photosphere. Thus, the turbulence parameters, often used as ad-hoc fudge parameters to enforce fits to observations, provide large uncertainty.

---

1) The specification given in Rutten and Van der Zalm (1984) contains printing errors. The formula in their Table II should read:
$x_1 = c_7 - 0.5\, c_5\, [\tanh(c_1(x_1 - c_2)) + 1] - c_6 \exp[-((x_1 - c_3)/c_4)^2]$.

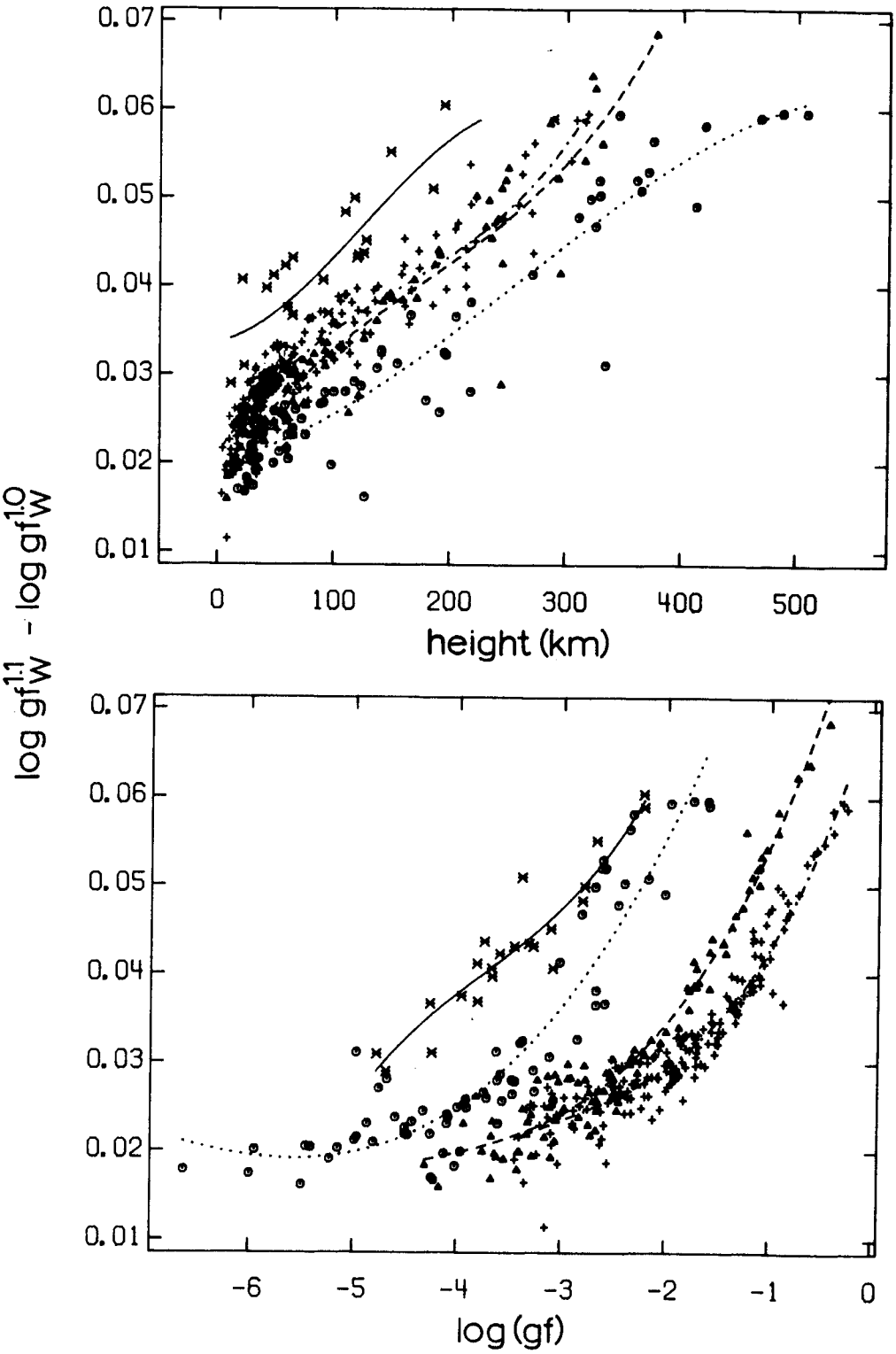

Fig. 4. Logarithmic differences between $gf_W^{1.1}$ and $gf_W^{1.0}$, i.e. the effect on the equivalent widths of a 10% (0.04 dex) increase on the computed continuous opacity, for the HOLMUL model and LTE, against height (top) and log(gf) (bottom). Other parameters and symbol coding as in Fig. 2.

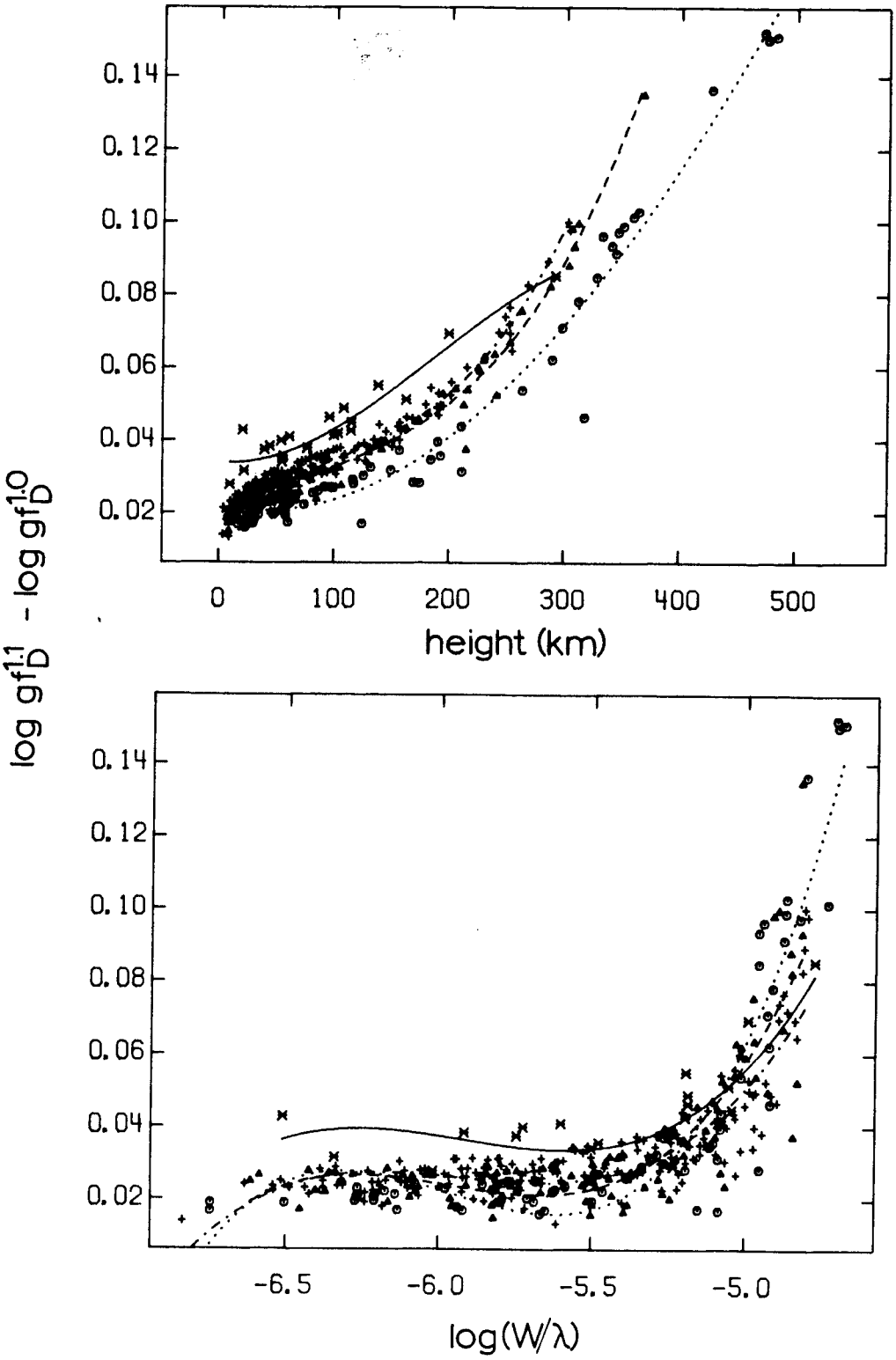

Fig. 5. Logarithmic differences between $gf_D^{1.1}$ and $gf_D^{1.0}$, i.e. the effect on the line depths of a 10% (0.04 dex) increase in the computed continuous opacity, for the HOLMUL model and LTE, against height (top) and the logarithm of the observed line strength (reduced equivalent width, bottom). Other parameters and symbol coding as in Fig. 2.

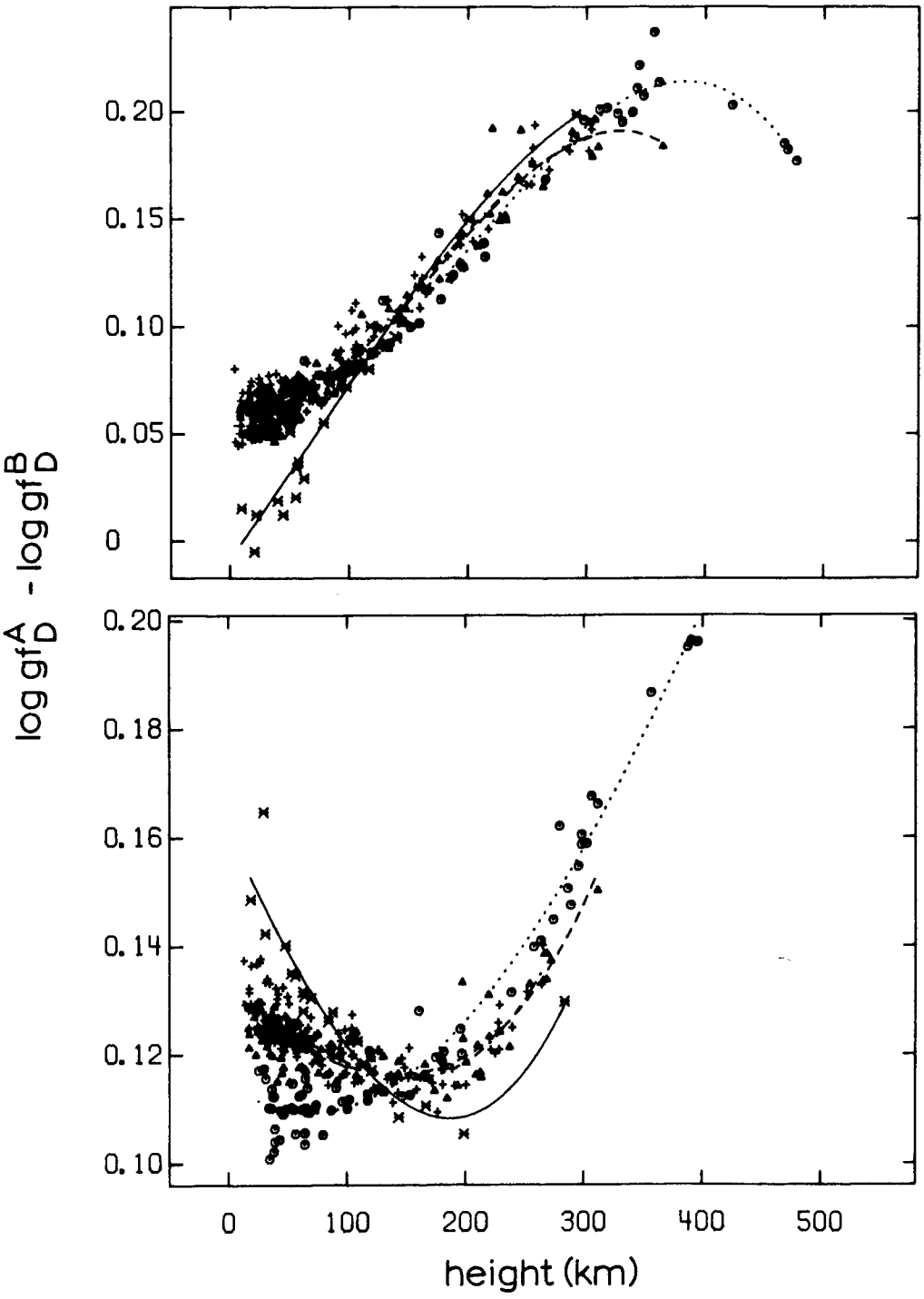

Fig. 6. Logarithmic differences between gf_D^A and gf_D^B for different microturbulence.
Top: HOLMUL model and LTE, gf_D^A for constant microturbulence (0.9 km/s) and macroturbulence = 1.75 km/s, gf_D^B for the height-dependent MACKKL microturbulence and macroturbulence = 1.3 km/s.
Bottom: HSRA model and NLTE, gf_D^A for Lites' (1973) vertical microturbulence and macroturbulence = 1.75 km/s, gf_D^B for the MACKKL microturbulence and macroturbulence = 1.3 km/s. Symbol coding as in Fig. 2

5. CONCLUSION

The various scatter diagrams show that empirical gf determination from the solar spectrum works - to some extent, and only for truly weak lines. The precision obtainable is about 0.1 dex or 25% at best, and one has to be careful about selection effects. The results depend sensitively on the ad-hoc choice of the turbulence parameters. Obviously, the advantage of solar gf-determination is that one obtains oscillator strengths for the lines needed. In addition, if other stars are like the Sun and the same computer program and assumptions are used, there may be even some fortuitous cancellation of errors in using solar values for stellar applications.

REFERENCES

Blackwell, D.E., Petford, A.D., Shallis, M.J., Simmons, G.J.: 1982, Mon. Not. R. Astr. Soc. 199, 43

Cram, L.E., Rutten, R.J., Lites, B.W.: 1980, Astrophys. J. 241, 374

Delbouille, L., Roland, G., Neven, L.: 1973, "Photometric Atlas of the Solar Spectrum from λ3000 to λ10000", Institut d'Astrophysique, Liège

Gingerich, O., Noyes, R.W., Kalkofen, W., Cuny, Y.: 1971, Solar Phys. 18, 347

Gurtovenko, E.A., Kostik, R.I.: 1981a, Astron. Astrophys. Suppl. 46, 239

Gurtovenko, E.A., Kostik, R.I.: 1981b, Astron. Astrophys. Suppl. 47, 193

Holweger, H.: 1967, Zeitschr. f. Astrophysik 65, 365

Holweger, H., Müller, E.A.: 1974, Solar Phys. 39, 19

Lites, B.W.: 1973, Solar Phys. 32, 283

Lites, B.W., White, O.R.: 1973, High Altitude Observatory Research Memorandum 185, Boulder

Maltby, P., Avrett, E.H., Carlsson, M., Kjeldseth-Moe, O., Kurucz, R.L., Loeser, R.: 1986, Astrophys. J. 306, 284

Moore, C.E.: 1959, Nat. Bur. Stand. US Techn. Note 36, "A Multiplet Table of Astrophysical Interest", US Dept. of Commerce, Washington, Revised Edition

Rutten, R.J., Kostik, R.I.: 1982, Astron. Astrophys. 115, 104

Rutten, R.J., Van der Zalm, E.B.J.: 1984, Astron. Astrophys. Suppl. 55, 143

Rutten, R.J., Zwaan, C.: 1983, Astron. Astrophys. 117, 21

Vernazza, J.E., Avrett, E.H., Loeser, R.: 1976, Astrophys. J. Suppl. 30, 1

Vernazza, J.E., Avrett, E.H., Loeser, R.: 1981, Astrophys. J. Suppl. 45, 350

Warner, B.: 1969, Observatory 89, 11